

# Design and Analysis of Indirect Solar Dryers for agriculture food product

Vijay R. Khawale  
Department of Mechanical Engineering,  
G.H. Raisoni college of Engineering and Management,  
Amravati. MS. India.  
e-mail: vijay.khawale@raisoni.net

Dr. Shashank B.Thakare  
Department of Mechanical Engineering  
Prof.Ram Meghe institute of technology and research,  
Amravati.  
e-mail: sbthakre2007@gmail.com

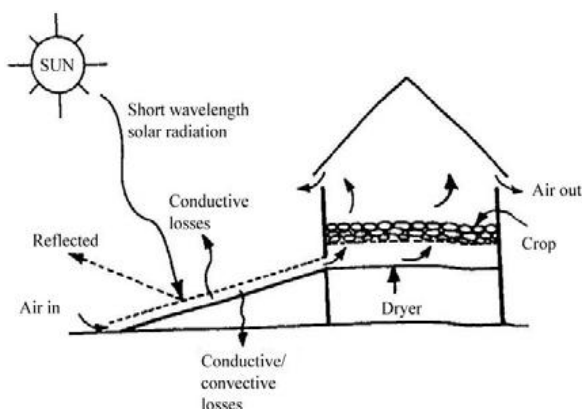
**Abstract** - The aim of the work is to cover a wide range of configurations and sizes with a simple indirect solar drier model. A model is developed to study the influence of design parameters such as collector dimensions and air mass flow rate on the performance of an indirect solar drier used for agriculture food product. In model the air is heated in the collector and the vapour mass transfer in the drying chamber. It is assumed that Constant rate of air flow controlled by convection mass transfer. The results show the significance of using a solar collector and the improvement of the drying process in the drying chamber. The available vapour mass flow rate is calculated for a variety of configurations, showing the incidence of the air mass flow and the sizes of the collector and the drying chamber. Temperatures during the process and the efficiency of the drying chamber are also illustrated.

**Keywords** - solar dryer, mass flow rate, agricultural food product, design parameter.

\*\*\*\*\*

## I. INTRODUCTION

The use of solar energy in drying applications is becoming an important and feasible alternative since it decreases consumption of conventional energy by 27–80% at an average solar collector system efficiency of 40% (Arata et al.1993). In addition, it can easily provide low temperature heating required for agricultural food drying applications (Mahapatra and Imre, 1990). Solar drying reducing the total amount of fuel energy required for the entire drying process. Normally natural convection solar crop dryers are perform inefficiently [1,2]. A various types of solar dryers are exist. A first classification is due to the nature of motion of the airflow. This can be natural convection or forced convection by means of a fan.



Working principle of indirect solar drying system (Sharma et al. 2009)[3]

Besides, solar dryers can be classified into direct, indirect or mixed depending on the parts of dryer exposed to solar radiation. In direct solar dryers, the product gets heated in a

chamber due to solar radiation through a transparent wall directly. Indirect solar dryers, a solar collector where the airflow is heated before being drive into the drying chamber. Mixed mode solar dryers combine both types, so solar radiation is absorbed by both.This work presents a theoretical study on the drying capacity of airflow for a wide range of design parameters, the solar collector performance and the relation of the drying chamber and the collector dimensions. The study focus on indirect solar dryer, The product to be dried in the trays of the drying chamber, and the air is forced to flow through the circuit.

## II. THEORY

The drying capacity of an airflow leaving the solar collector depends on its relative humidity and its mass flow rate. Thus, if the air is heated in a collector, the temperature increase and a relative humidity decrease and vapour absorbing capacity of airflow increase. Assuming steady state conditions, the temperature of the airflow leaving the solar collector depends on the solar irradiance over the collector area, the collector efficiency and the mass flow rate. Energy balance equation shows;

$$ma \cdot Cpa(Tc - Ti) = \eta AG \quad (1)$$

Where A=collector area (m<sup>2</sup>); Cpa=specific heat of air at constant pressure(J/ kg °C); G=solar incident on the collector(W/m<sup>2</sup>); ma=air flow rate ( kg/s); ti= temperature of the inlet air (°C); anf tc=temperature of the outlet air (°C). The expression for collector efficiency is given as [2]:

$$\eta = Fr \cdot (\tau\alpha) - Fr \cdot Ul \frac{Tc - Ti}{G} \quad (2)$$

Fr is a heat removal efficiency factor. It is the ratio of actual heat gain to the heat gain that would result if

the temperature of the airflow at outlet of the collector is equal to absorber temperature. It depends on the type of collector and the mass flow rate, and it has to be experimentally determined. In present study, Fr is assumed constant. This is, independent from ma, UI can also be assumed constant [4]. The optical properties, transmittance  $\tau$  depend on the material of cover and absorptance  $\alpha$ , depend on the materials of the absorber. The paper is presented to scope a wide range of types of solar dryers and overall values have been taken on literature based for these parameters and assumed constant. Therefore, from equation 1 and 2:

$$T_c = T_i + \frac{Fr.\tau\alpha}{\frac{C_p a.m_a}{G.A} + \frac{Fr.U_l}{G}} \quad (3)$$

The air density and specific heat are assumed constant as the variation of temperature in a working range is too small. During this process specific humidity remains constant as no water is added or extracted. The air leaving from the collector is driven to the drying chamber [Fig.1], where the drying process occurs. The drying process is assumed to be adiabatic (and thus isenthalpic for the airflow). psychrometric equations are used for making model of drying process. The saturation conditions of the airflow leaving the drying chamber shows a maximum sorption and will be obtained from the equation given below (4):

$$\omega_o.sat[hg + Cpv(T_o.sat - T_o)] = Cpa(T_c - T_o) + \omega_{in}[(hg + Cpv(T_c - T_o))] \quad (4)$$

The air leaving the chamber is saturated, denoted by sun-index sat. This will shows a maximum drying effect in the drying chamber (as for an infinite chamber). Saturation is a optimum condition of drying air that would be reached or not at outlet of drying chamber depending on the dynamics of the process. The maximum mass flows of vapour that can be absorbed by the airflow represent the drying capacity. This is equal to the product of air mass flow and the specific humidity difference between ambient conditions and saturation, From eq.4 present parameter calculated..

$$mv = ma(\omega_o, sat - \omega_c, in) \quad (5)$$

In order to find the heat energy required to vaporize the water, drying capacity should be multiplied by enthalpy of evaporation of water (hfg). Results are compared with the total solar power entering the collector:

$$Mv = \frac{mv.hfg}{G.A} \quad (6)$$

The design and analysis of drying process along the drying chamber has been done for achieving the maximum vaporization. The drying rate depends on the mass transfer from the surface or by unsaturated surface and internal mechanism of liquid flow In the first case, it is assumed that a sufficient water supply to the surface from the internal

structure of the drying material and the process will be controlled by the mass convection rate from the surface to the airflow only. In the second case, the flow rate of internal moisture to the surface is controlling the process dynamics. Study is mainly focused on mass transfer process controlled by the mass convection rate. The vapour mass flow is given by [8]:

$$mv = KAd(\omega_{sat} - \omega_d) \quad (7)$$

K and Ad are the convective mass transfer coefficient and drying surface respectively.  $\omega_{sat}$  is the specific humidity for saturation conditions at the surface temperature, and  $\omega_d$  the specific humidity of the airflow in drying chamber. From the energy balance equation at drying surface the surface temperature  $T_s$  is obtained (neglecting conduction and radiation terms). Steady state is assumed

$$hc(T_d - T_s) = K(\omega_{sat} - \omega_d)hfg \quad (8)$$

Convective mass transfer coefficient (K) and heat convection coefficients (hc) in eq.8 can be calculated from equation 9 [5] for turbulent flow.

$$\frac{hc}{C_p a.\rho u} Pr^{\frac{2}{3}} = \frac{K}{\rho u} Sc^{\frac{2}{3}} = 0.11 ReD^{-0.29} \quad (9)$$

Where ReD is the Reynolds number referred to the hydraulic diameter of the cross-section. Eq.8 is only valid for internal turbulent flow ( $2600 < ReD < 22000$ ). Along the length of the drying chamber the temperature of the airflow  $T_d$  and the temperature of the drying surface  $T_s$  can be determined.

### III. ANALYSIS

The problem was separated in two parts. 1. Analysis of the collector performance, 2. Analysis of the drying process on agriculture product in the drying chamber. The first part analyse the drying capacity of the system, while the second one studies the effect of drying chamber dimensions and arrangement on the drying process. The results are used to use to study the correlation between the collector and drying chamber in order to define design parameters. Steady state conditions were considered.

The collector performance was analysed in terms of the collector efficiency and the final temperature of the airflow rose. The collector dimensions and the air mass flow rate are varying parameter. Aggregating the relevant parameters, a single variable, mass flow rate per unit of collector area  $ma/A_c$  was used. For the present results ambient conditions are set to be 28°C, 61% relative humidity and a solar irradiance of 4.81KWh/m<sup>2</sup>/day, which represent average tropical conditions of city Amravati, MS, India. After the study of collector performance, the drying capacity of the airflow can be calculated as a function of  $ma/A_c$ .

The drying chamber performance is analysed using a numerical methods. The length of the drying path is divided into differential elements ( $N \sim 10^3$ ). Based on the energy balance equation (eq.8), by using an iterative method the air

and surface average temperatures are calculated for each element. The initial air temperature is measured at the inlet of the element (inlet of the drying chamber for the first element). With that temperature, for the first element it is calculated from eq.8. Then, the air temperature leaving the differential element is calculated using an energy balance equation and the average air temperature is set. As the process settled, it is repeated in the next differential element following an upwind scheme along the drying path. Thus the temperature distributions of the airflow and the surface are found. The range of deviation of the key parameters ought to be recognized, and some are given a same value for this preliminary work. In literature an investigation was done in search of the common working range. for indirect solar dryers For the indirect solar dryer the interested range of  $ma/Ac$  is  $10^{-3}$  to  $10^{-1}$   $kg/(s \cdot m^2)$  [6]-[9]). This is the only parameter affecting the collector analysis. For drying chamber analysis, other restrictions are necessary. To obtain the airflow velocity in the drying chamber some geometrical parameters in both collector and drying chamber have to be set. Then, the interval of  $ma/Ac$  should be set to cope the limitations of eq.9. Then conditions for the drying chamber calculations are follows: such as collector length,  $L$ , is put to 1.5m., collector and drying chamber airflow cross sections (between trays) are the same ( $W=W_d$  and  $s=s_d=0.1m$ ). Therefore, air velocities are varied between 0.2m/s and 2m/s, and  $ma/Ac$  ranges between 0.001  $kg/(s \cdot m^2)$  and 0.2  $kg/(s \cdot m^2)$ .As per the literature upper part of the working range found in the collector calculations is comparable. In order to fit the lower range, for natural flow applications, a natural flow correlation for the mass and heat flow should be used.

#### IV. RESULTS

In this section, the drying capacity of the airflow is found after the calculations.

1.The collector performance is analysed in terms of outlet temperature and the maximum vapour mass flow. 2.The drying chamber performance is analysed.

##### I. Collector performance

The air enters the solar collector at ambient conditions in the solar collector and is heated. The air leaving the collector is immediately driven into the drying chamber. Form Eq.3 the temperature at the outlet of the collector is calculated which is a function of air mass flow rate per unit of collector area, is shown in Fig.2. Eq.3 shows a linear effect of a Solar irradiation on the temperature of air flow in the collector. Therefore, changes on the solar irradiance gives a linear

variations in the presented temperature.

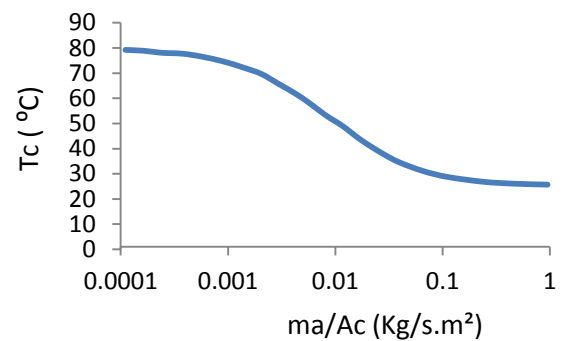


Fig.2. Temperature of air at collector outlet with mass flow rate.

Results show for a wide range of mass flows and collector areas (Fig.2), ensuing with the range previously selected. A maximum temperature is approached for low mass flows per unit collector area and a low efficiency on the collector due to high heat losses, as shown in eq.3. For large  $ma/Ac$  values there is a negligible increase in temperature, as heat per unit of mass is small. In this case the efficiency of collector would be high, as losses are small (low collector temperature), but no significant temperature addition is achieved, and thus there is no considerable relative humidity decrement. Therefore, the collector is useless. In the intermediate zone both the collector efficiency and the temperature increase are relevant and intermediate. In Fig. 3 shows the maximum drying capacity can be obtained from such airflow. In this graph the dimensionless variable presented in eq.6 is describe and found that the actual drying capacity also depends on irradiation and collector area. Cases with and without the solar collector are

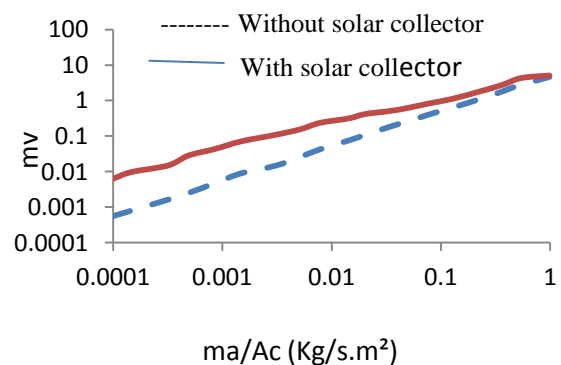


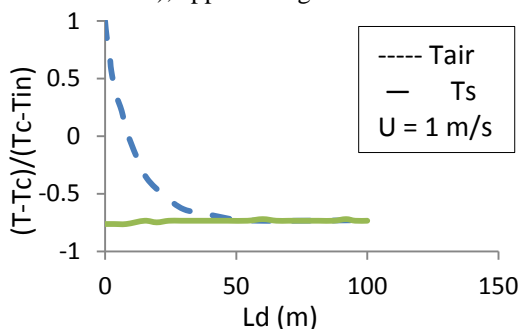
Fig.3. Maximum vapour mass flow rate with air mass flow per unit c/a of collector.

shown for a wide range of air mass flow per unit of collector area. The airflow enters directly to the drying chamber without collector and thus the drying process begins at ambient temperature is depicted for comparison. The curves in Fig.3 show a proportional trend with the mass flow rate. The effect on drying without collector is that doubling the vapour mass rate by doubling the air mass flow rate [10]. In

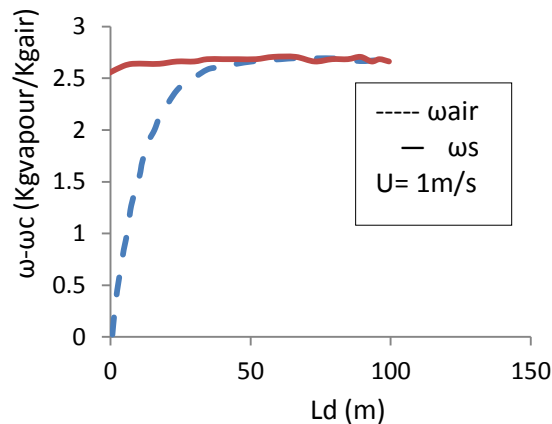
the collector case, the temperature of air flow increases which modifies the air mass flow effect. The temperature of airflow increase in the collector due to which a specific humidity changes in the drying chamber from inlet chamber conditions to saturation condition. When the mass flow rate per unit of collector area is low, the use of the collector improves the drying capacity, as an significant temperature increase in the solar collector is obtained, and thus an increment in specific humidity can be achieved. The result is that in the range of  $10^{-3}$  -  $10^{-1}$   $\text{kg}/(\text{s}\cdot\text{m}^2)$  the vapour mass flow rate is not proportional to the air mass flow rate. Below  $10^{-3}$   $\text{kg}/(\text{s}\cdot\text{m}^2)$ , the effect of the collector is maintained, but the proportional effect of the air mass flow reappears. These two effects explain that most dryers work in this range. The special interest for forced convection dryers is an increase of the vapour mass rate but that is not directly a result of increasing the airflow using of fan power. When the mass flow is too large for the collector area, no temperature increment is achieved and the results with and without collector collapse.

## II. Drying chamber performance

Results for the drying process are calculated for a air velocities ranges between 0.2 and 2m/s, and  $m_a/A_c$  between 0.001 and 0.2  $\text{kg}/(\text{s}\cdot\text{m}^2)$ , and with a fixed dimensions of both collector and drying chamber. Figure 4 shows the temperatures and specific humidity's along the drying chamber that control the drying process (eq.8). Note that the calculations rely on the total length available for heat and mass transfer between the product and the airflow and valid up to the correlations of eq.9 can be accepted. Results are presented in dimensionless terms, and for an intermediate value of airflow velocity of 1 m/s. As the airflow moves along the drying length its moisture content increases and its temperature decreases (adiabatic process has been assumed), approaching the wet bulb



(a)



(b)

Fig.4.a&b shows surface and air flow temperatures and relative humidities along the drying chamber.

The surface temperature and its specific humidity for saturated conditions is determined by the heat balance equation (eq.8). The results show an almost constant surface temperature. For large lengths, air and surface conditions merge and the drying process stops. The amount of vapour mass absorbed from surface by the airflow decreases along the chamber. This observation is help for designing the economical drying chamber dimensions. The temperature graph shows the evolution of both the airflow and the surface temperatures. The dimensionless temperature parameter is the difference of these temperatures with ambient temperature compared to the temperature increment in the solar collector [10]. Therefore, negative values represent temperatures lower than the ambient temperature. As the air flows along the dryer it losses heat, used to evaporate the water on the product surface, and thus its temperature decreases. The specific humidity evolution is presented as the increment in specific humidity of air from ambient conditions. Both graphs shows that the airflow temperature and humidity change mainly in the first 20 meters, and reach saturation values around 40 meters for this specific configuration.[10]

From the results of Fig.4, the vapour mass flow can be calculated using eq.7. It can be compared with the maximum vapour mass flow depicted in Fig.3, which is the drying capacity of the airflow to saturation and corresponds to the case for  $L_d \rightarrow \infty$ . An efficiency of the drying chamber can thus be defined in the form:

$$\frac{mv(L_d)}{mv(\infty)}$$

$T_{air}$  -----  
 $T_s$  -----  
 $U = 0.95 \text{ m/s}$

For different drying chamber the effect of the efficiency are presented in Fig.5

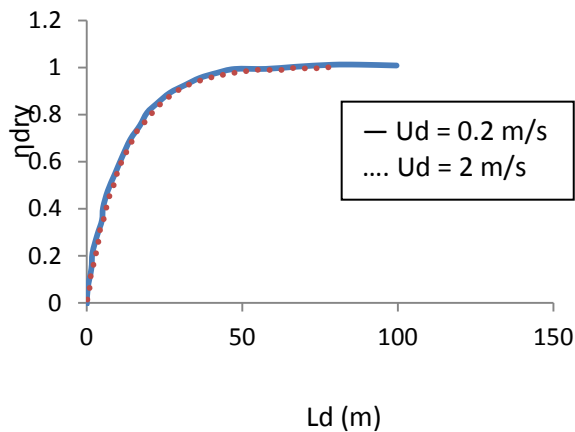


Fig.5. Drying efficiency along the length of drying chamber

Fig.5 shows that for maintaining the same efficiency if airflow velocity decreases then the drying chamber dimensions are also reduced due to the dependence on the velocity of the mass and heat convection coefficients. Both coefficients, disregarding the minor effect of the variation of the Schmidt number (as the diffusion coefficient varies with temperature) are a function of  $u^{0.71}$  (see eq.8). The maximum vapour flow rate varies with the mass flow, as established in Fig.3. Combining the results on Fig.3 and Fig.5, the mass flow rate of vapour was obtained as a function of the air mass flow rate per unit of collector area, and for different lengths of the drying chamber. The results are shown in Fig.6.

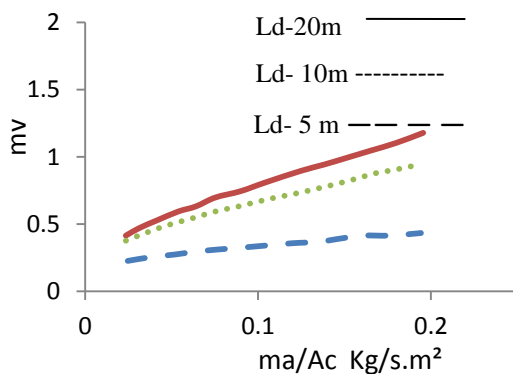


Fig.6. Vapour mass flow rate vs. hot air mass flow rate at drying chamber.

From the dimensionless variable depicted in Fig.6, the dimensional vapour mass flow rate can be obtained using eq.6. [10]. The solid line represents the maximum vapour mass flow previously represented in Fig.3, but for the range of study here, which is  $2 \cdot 10^{-2}$  to  $2 \cdot 10^{-1}$   $\text{kg}/(\text{s} \cdot \text{m}^2)$ . Thus the vapour mass rate is not proportional to the air mass flow, but a factor 10 increase of the air mass flow results in an approximately factor 3 increase of the vapour mass rate. An increase of the collector area would be a solution in such

cases. Figure 6 contain three dotted-dashed lines represent the results for drying chambers of different dimensions and shows the effect of the air mass flow rate on drying chamber lengths. For a 5 m drying chamber, the effect of the air mass flow is rather small, factor 10 increases of the air mass flow producing a factor 2 increase of the vapour mass rate. This is reduced the residence time of the air in the drying chamber. The large air mass flows and small drying chamber will result the unsaturated airflow at outlet of the drying chamber which will reduce the drying efficiency.

## V. CONCLUSIONS

This work presents a model of the main processes occurring in an indirect solar dryer for agriculture food drying. The main design parameters of model are the airflow velocity and the dimensions of the solar collector and the drying chamber. The performance of solar collector depends on the air mass flow rate per unit of collector area. The collector performance identify the drying capacity of the airflow in the region where the effect of the air mass flow diminishing, which is proportional to the vapour mass rate in the zones where the collector is not well design..However, a high airflow velocity yields a low residence time in the drying chamber, a factor that could result in low drying efficiency, as the airflow would not have time to saturate, losing part of its drying capacity. Air mass flow rate, collector area and drying chamber length are the significant parameters in the design of an indirect solar dryer. The air mass flow rate is more relevant factor which can be controlled by fan power, but it adds to the cost of the dryer. The air mass flow rate depends on the drying chamber length and geometry. A small length may result in low drying efficiency due to west of drying capacity of airflow and large length resulting in increase of cost.

## Nomenclature

A	collector area ( $\text{m}^2$ );
Cpa	specific heat of air at constant pressure ( $\text{J}/\text{kg} \cdot ^\circ\text{C}$ );
G	solar incident on the collector ( $\text{W}/\text{m}^2$ );
ma	air flow rate ( $\text{kg}/\text{s}$ );
Ti	temperature of air at the inlet of collector ( $^\circ\text{C}$ );
Tc	temperature of air at the outlet of collector ( $^\circ\text{C}$ ).
Ad	Drying surface area. ( $\text{m}^2$ )
Cpv	Vapour specific heat ( $\text{J}/(\text{kg} \cdot \text{K})$ )
Fr	Heat removal factor
hc	Heat convection coefficient ( $\text{W}/\text{m}^2\text{K}$ )
hfg	Vaporization enthalpy ( $\text{J}/\text{kg}$ )
hg	Enthalpy of saturated vapor at $0^\circ\text{C}$ ( $\text{J}/\text{kg}$ )
K	Convective mass transfer coefficient. ( $\text{kg}/\text{s} \cdot \text{m}^2$ )
L	Solar collector length (m)
Ld	Drying chamber length (m)
mv	Vapour mass flow ( $\text{kg}/\text{s}$ )
Pr	Prandtl number
Red	Reynolds based on hydraulic diameter
S	Solar collector thickness (m)]
Sd	Space between trays (m)
Sc	Schmidt number

To	Reference temperature 0°C (K)
To sat	temperature of saturated air at the drying chamber outlet (K)
Tref.	Reference temperature 28°C (K)
Ts	temperature of the surface of the product (K)
Td	temperature of air in the drying chamber (K)
u	Airflow velocity in the collector (m/s)
Ud	Airflow velocity in the drying chamber (m/s)
W	Solar collector width (m)
Wd	Solar dryer width (m)
$\alpha$	Absorptance
$\eta$	Solar collector efficiency
$\eta_{dry}$	Drying efficiency of the drying chamber
UI	overall heat loss coefficient
$\omega_{in}$	Specific humidity of air at the solar collector inlet (kgvapour/kgair)]
$\omega_{sat}$	Specific humidity of saturated air at the drying chamber outlet (kgvapour/kgair)
$\omega_{sat}$	Specific humidity for saturation conditions at the surface temperature (kgvapour/kgair)
$\omega_d$	Specific humidity of saturated air at the drying chamber outlet (kgvapour/kgair)
$\rho$	Air density (kg/m <sup>3</sup> )
$\tau$	Transmittance

[10] L. Blanco-Cano, A. Soria-Verdugo, L.M. Garcia-Gutierrez and Ruiz-Rivas. Modelling and Design of indirect solar dryers for batch drying, 2013. International conference on Renewable Energy and power quality,

#### REFERENCES

- [1] Ekechukwu OV, Norton B. Design and measured performance of a solar chimney for natural circulation solar energy dryers. *Renew Energy* 1997;10: 81-90.
- [2] Ekechukwu OV. Review of solar-energy drying systems II: an overview of solar drying technology. *Energy Convers Manag* 1999;40:616-55.
- [3] Sharma, A., Chen C., Nguyen Vu Lan., 2009, Solar-Energy Drying Systems: A Review. *Renewable and Sustainable Energy Reviews*, 13, pp. 1185–1210.
- [4] Duffie, J.A., Beckman W.A., 2006. “Solar engineering of thermal processes”. 3rd Edition. John Wiley & Sons
- [5] Treybal R.E., 1987 “Mass-Transfer Operations”. 3<sup>rd</sup> Edition. McGraw Hill
- [6] Bolaji B.O., 2005. Development and performance evaluation of a box type absorber solar air collector for crop drying. *Journal of food technology*, 3, 595-600.
- [7] Karim, M.A., Hawlader, M.N.A., 2004. Development of solar air collector for drying applications. *Renewable Energy*, 32, 1645-1660.
- [8] Pangavhane, D.R., Sawhney, R.L., Sharsavadia, P.N., 2002. Design, development and performance testing of a new natural convection solar dryer. *Energy*, 27, 579-590.
- [9] Madhlopa, A., Jones, S.A., Saka, J.D.K., 2002. A solar air heater with composite absorber system for food dehydration. *Renewable Energy*, 27, 27-37